

CO-OP WORK TERM REPORT
SUMMER 2004:

**The Design and Construction of
Single-Stage and Dual-Stage
Photodetectors**

by Jordan Baglo

Submitted September 7, 2004.

SN: 39481023
PHYS 298

Employer: Dr. Kirk Madison

The Design and Construction of Single-Stage and Dual-Stage Photodetectors

Jordan Baglo
SN: 39481023

September 7, 2004

I Preface

This report is a very broad overview of the design, construction, and testing of two different models of photodetectors which I carried out during the months of May through to September, in my Co-op work term placement in the laboratory of Dr. Kirk Madison of the UBC Department of Physics. During my work term I was also assigned other individual projects, including the design and construction of the power supply boxes that will be used as the primary power source for much of the laboratory equipment being built (including these photodetectors). I also made contributions to many other laboratory projects, such as a voltage regulator circuit and a diode laser protection circuit, with which I had various degrees of involvement. However, I spent the majority of my time and effort throughout the term working on the photodetectors, and I have decided to write my work term report on the single-stage and dual-stage photodetectors for this reason.

In this report, I will briefly discuss the field of research and type of experiment being conducted in the lab, placing the photodetectors in this context. After the introductory content, I will describe the initial evaluation of the operational amplifier used in the photodetector circuit, as well as the radio-frequency (RF) design problems—and solutions—that were encountered. Next follows a detailed description of the construction of the original single-stage photodetector, and the methods that I used to evaluate the photodetector’s performance. Finally, the issues involved in the design and construction of the dual-stage photodetector are discussed, and the development process for the two-stage detector is outlined.

I must stress that, although the coverage of this report ends with its final submission, the photodetectors are still very much works in progress. Not only do the detectors need to be “mass produced,” in quantities beyond the single prototypes being considered for this project, but many modifications and improvements to the designs of the the detectors are pending as well. The designs of the photodetectors (particularly the dual-stage model) are continuously evolving, and may continue to change with the requirements placed on them by the experiment.

For their contributions to both the photodetector project and this report, I would like to thank the members of my lab—Dr. Madison, Dr. Bruce Klappauf, Janelle van Dongen, Amy Liu, and Tao Kong. I am especially grateful to Dr. Madison for providing me with the opportunity to work on this project, as well as for his guidance with the design of the circuits, and his thorough explanations of the “big picture” of the experiment. Dr. Klappauf provided me with much assistance with testing my circuits, especially with troubleshooting my early op amp stability problems. Janelle, Amy, and Tao were always ready and willing to help me with my circuit construction, to suggest ideas for this report, or just to provide moral support. My project has been made much less difficult—and much more enjoyable—with the assistance of all my group members, and it is to them I owe thanks for my great experience this summer.

Contents

I	Preface	ii
1	Introduction	1
	1.1 The Research	1
	1.2 The Detectors	2
2	The Single Stage Photodetector	3
	2.1 Initial Design	3
	2.2 Preliminary Evaluation of the OPA686 Op Amp	4
	2.3 Building the Single-Stage Photodetector	7
	2.4 Measuring the Frequency Response	8
	2.5 Conclusion	12
3	The Dual-Stage Photodetector	13
	3.1 Introduction	13
	3.2 The Circuit Design	13
	3.3 The Board Layout	16
	3.4 Building the Dual-Stage Photodetector	17
	3.5 Conclusion	18
	Appendices	19
A	The Operational Amplifier	20
	A.1 Basic Uses and Properties	20
	A.2 Negative Feedback and the “Golden Rules”	20
	A.3 The Inverting Amplifier	21
	A.4 The Noninverting Amplifier	22
B	The Laser Lock System	23
	B.1 Doppler-free Saturated Absorption Spectroscopy	23
	B.2 Phase Sensitive Detection	23
C	The Photodetector Enclosure	25
D	List of Equipment	29
	D.1 Design and Data Analysis Software	29
	D.2 Electrical/Optical Measurement Equipment	29
	D.3 Laser Equipment	29
	D.4 Power Supplies and Signal Sources	30
	D.5 Soldering and Assembly Equipment	30
	D.6 PCB Processing Equipment and Supplies	30
E	List of Vendors	31
	Bibliography	32

List of Figures

1	Velocity distribution of the first BEC	1
2	The original photodetector design.	4
3	The OPA686 on a “Surfboard” surface mount adaptor.	5
4	An assembled photodiode amplifier.	8
5	The original frequency response data with the LED	9
6	Several LED-measured frequency responses.	10
7	A comparison with a Thorlabs detector.	11
8	The dual-stage photodetector schematic.	15
9	Both sides of the circuit board trace.	16
10	A fully assembled dual-stage photodetector board.	17
11	The inverting and noninverting amplifiers	21
12	Photodetector enclosure design, overview	25
13	Photodetector enclosure design, front panel	26
14	Photodetector enclosure design, bottom plate	27
15	Photodetector enclosure design, top plate	27
16	Photodetector enclosure design, rear plate	28
17	Photodetector enclosure design, side panels	28

List of Tables

1	Electronics, CAD, and analysis software used.	29
2	Measurement equipment used.	29
3	Laser equipment used for testing.	29
4	Power supplies and signal sources used.	30
5	Soldering and assembly equipment.	30
6	PCB processing chemicals and equipment.	30
7	A list of vendors, distributors, and other businesses used	31

1 Introduction

1.1 The Research

This project takes place in the laboratory of Dr. Kirk Madison, of the Department of Physics at the University of British Columbia. The focus of the group's research, which falls both in the fields of atomic, molecular, and optical (AMO) physics and in condensed matter physics, is that of Quantum Degenerate Gases.

1.1.1 Bose-Einstein Condensation

In short, the study of Quantum Degenerate Gases involves the production of ultra-cold atomic gases, and the highly non-classical phenomena which occur in systems of such gases. The most well-known example of such a system is the Bose-Einstein Condensate (BEC). Although Bose-Einstein condensation was predicted by Albert Einstein¹ in 1924, the phenomenon was not observed until June 1995, when Eric Cornell and Carl Weiman created the first BEC at JILA (at the University of Colorado, Boulder) in a gas of ^{87}Rb atoms (see Figure 1).

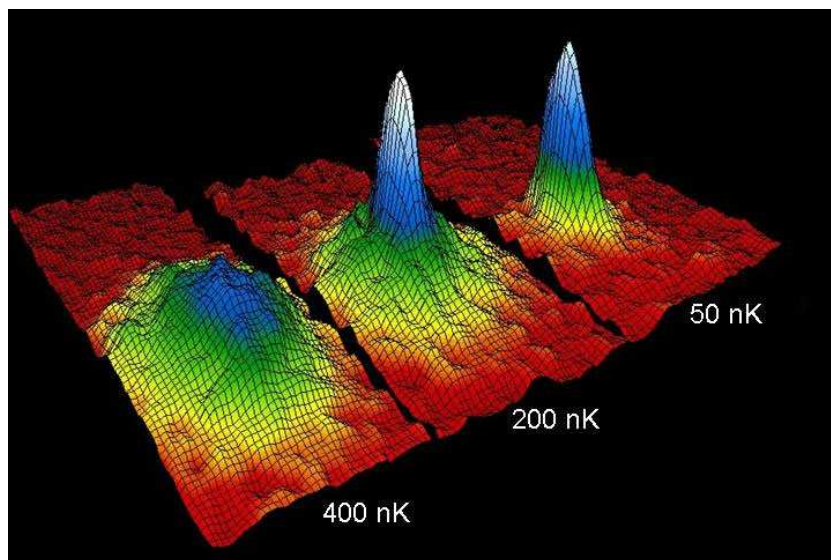


Figure 1: A computer-generated image of the velocity distribution of the first observed Bose-Einstein condensate at JILA. This image is from the JILA website, at <http://jilawww.colorado.edu/bec>.

The phenomenon of Bose-Einstein condensation occurs when bosonic atoms

¹Einstein's work was based on the noninteracting particle statistics ideas of Satyendra Bose, which are now known as Bose-Einstein statistics; Bose himself played no direct rôle in Einstein's prediction of the BEC [1].

(those with integer spin) are cooled sufficiently low, typically on the order of hundreds of nanokelvin², such that the density of atoms with a given energy near the ground state becomes extremely high. When cooled below some critical temperature T_c , some atoms coalesce into the ground state, with all of the atoms condensing together into the ground state in the limit as $T \rightarrow 0$ [1].

What is remarkable about this condition is that the ground-state rubidium atoms—which being bosons, are not subject to the Pauli exclusion principle—have the exact same quantum state; they become a single, massive particle described by a single wavefunction! Such Bose-Einstein condensates can be made to have more than 10^6 atoms, and can have lifetimes in the tens of seconds [13]. These macroscopic³ quantum systems provide an unprecedented opportunity to *directly* manipulate and observe quantum phenomena in the laboratory, providing a veritable scientific “playground” for the experimentation with quantum and condensed matter systems that had been inaccessible for decades. The construction of a rubidium BEC is among the first goals of this group.

1.1.2 Degenerate Fermi Gases

Although such condensates of bosonic atoms provide excellent experimental opportunities for the study of many quantum phenomena, the study of ultra-cold fermions is also of much interest. Due to the Pauli exclusion principle, no more than one fermion can occupy the same quantum state (when opposite spins are considered to be different states), and thus no exact fermionic equivalent of the Bose-Einstein condensate can be obtained. However, ultra-cold gases of fermions exhibit their own degenerate, highly-correlated behaviours (such as Cooper pair formation) [10]. The study of such such behaviours in degenerate Fermi gases will prove invaluable for testing condensed matter theories—particularly those pertaining to high T_C superconductivity—which involve systems of fermions such as electrons.

One method of obtaining such ultra-cold systems of fermions is to use a Fermi-Bose mixture, a mixture of fermions and bosons. By first creating a BEC with the bosons in the mixture in the same manner as usual, the fermions are cooled by the BEC, beyond what is typically possible with other techniques using fermions alone [10]. This method of sympathetic cooling will be applied in this lab—using ^{87}Rb as the bosonic species and ^6Li as the fermionic species—to create and study such systems of degenerate Fermi gases.

1.2 The Detectors

1.2.1 General Applications

The photodetectors were not designed for (nor shall they be dedicated to) a single application in the laboratory; rather, they were designed to be used in many different situations in which light needs to be measured or monitored.

²Using laser cooling and magneto-optical traps; see [12], for example

³Macroscopic, that is, for a quantum system!

The countless possible uses of the detectors will require of them the ability to measure light signals with a wide range of characteristics, from weak to intense, and from steady to high-frequency; this needed versatility places constraints on the design of such a general-purpose photodetector.

One of the most common—and least technically demanding—uses of the photodetectors will be the monitoring of the light intensity of the direct⁴ laser beams. The detectors will also be used to measure the fluorescence of the trapped atoms, as well as that of the cold atom beams. The photodetectors may additionally be used as part of a Fabry-Perot interferometer, used to monitor the wavelength of the beams.

1.2.2 The Laser Locking System

Although the detectors will not be used for just a single purpose, there is one application which stands out as among the most important: the laser locking system. This locking system uses the techniques of Doppler-free saturated absorption spectroscopy and phase-sensitive detection to provide the necessary feedback loop to lock the laser wavelengths to the desired atomic line. For a brief discussion of these techniques, see Appendix B.

In terms of the requirements the locking system places on the photodetectors, since the piezoelectric element will modulate the AOM at roughly 100 kHz, it will be necessary for the photodetectors to have frequency responses well above this range. Additionally, since the changes in light intensity on the photodetectors due to absorption of the beam will be small, high-frequency modulations riding on large offsets, it would be useful to produce a detector that only amplifies this modulation. These issues have been dealt with in the construction of the photodetectors, which is the subject of this report.

2 The Single Stage Photodetector

2.1 Initial Design

The original plan for the photodetector was based on a design by Todd Meyrath of the University of Texas at Austin [8]. This basic design (see Figure 2) utilizes a high-speed photodiode together with a high speed operational amplifier, with the aim of producing a high-speed photodetector unit.

The operational amplifier that was chosen was the Burr-Brown OPA686. This op amp has an extremely high gain-bandwidth product ⁵ of 1600 MHz; for comparison, typical general-use op amps have bandwidths in the tens of megahertz and under. Although the high bandwidth will allow the detection of

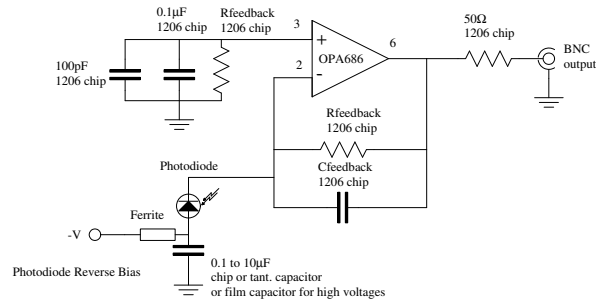
⁴The “direct” beams may have first been split, filtered, polarized, or otherwise attenuated; for sufficiently intense beams, neutral density filters will be necessary to prevent the beam from saturating the photodiode and the output of the operational amplifier, in order to keep the measurements in the linear regime of the photodetector.

⁵Commonly known as the unity-gain bandwidth, f_T , which is the bandwidth at a gain factor of one; for op amps that are not stable at a gain of one, this value is interpolated.

PHOTODIODE AMPLIFIER

Based on the sample design from the OPA686 datasheet

Todd Meyrath
Oct 2003



Power Supply Bypass

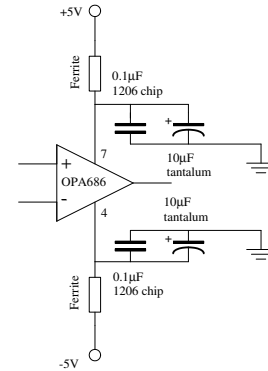


Figure 2: The original photodetector design, by Todd Meyrath [8].

a greater range of signals, thus producing a more versatile detector, the op amp will also be more vulnerable to noise and self-induced oscillations than slower operational amplifiers. These problems were encountered—and dealt with—during the course of the project, and are discussed in the report below.

The operational amplifier will be used in a transimpedance configuration, which is essentially a current-to-voltage converter. The feedback resistor from the op amp’s output to its inverting input sets the “transimpedance gain”. Whatever current is input into the transimpedance amplifier will be produce an output voltage according to Ohm’s law, helped along by the output of the op amp; that is, $V_{out} = I_{in}R_f$, where R_f is the transimpedance gain. This enables components like the photodiode, which are unable to produce the necessary large voltages to “enforce” their current output across heavy loads, to produce voltages large enough for easy observation with an oscilloscope⁶. This is essentially the nature of the photodetector circuit to be built.

2.2 Preliminary Evaluation of the OPA686 Operational Amplifier

Before designing the full photodetector, it was decided that a test of the performance and characteristics of the workhorse of the photodiode amplifier circuit, the Burr-Brown OPA686 operational amplifier, would provide useful insight for the detector design. A simple test circuit which used the op amp in an inverting

⁶More details about op amps may be found in Appendix A, and in [6]

amplifier configuration⁷ was to be set up for this purpose. The power supply connection—complete with decoupling capacitors—was set up the same as in the intended final design (see Figure 2, on the right), and the gain was set to be 20 through the use of a 1 k Ω feedback resistor and a 50 Ω input resistor (see Section A.3).

2.2.1 Early Breadboard Testing

The first attempt at construction of this test circuit was performed on a breadboard. The OPA686 (and most of the other components that will be used in this project) is a surface mount component; in particular, it has an SOIC-8⁸ package. Such components are typically very small, and have no “through-hole” leads for which holes must be drilled in a board; rather, these components are electrically connected to the board by soldering tiny contacts or leads to pads on the board. The only way to test such components on a breadboard is to solder them to an adaptor board (a “Surfboard,” see Figure 3) with pads designed for an SOIC-8 footprint connected to corresponding SIP pins (“Single Inline Pins,” with 0.1” pitch) that fit into common breadboards.

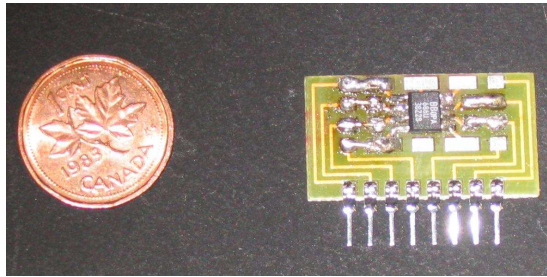


Figure 3: The minuscule OPA686 on a “Surfboard” surface mount adaptor. Note the size comparison with the penny!

In early testing, the Surfboard on which the OPA686 was soldered was plugged into a breadboard, on which all of the inputs, outputs, power supply connections (with ferrite filters and decoupling capacitors) and feedback components were arranged, using standard through-hole components. When this inverting amplifier test setup was evaluated by using a sinusoidal signal from a function generator, the results were found to be extremely unsatisfactory; the amplifier (with few exceptions) did not work. Most of the time, the output signal consisted of wild, full-scale oscillations which appeared essentially uncorrelated with the input signal, and seemed to be the result of some sort of self-resonance property of the op amp itself.

⁷The inverting amplifier was chosen for testing purposes because it matches most closely the transimpedance amplifier configuration to be used; the inverting amplifier is essentially a transimpedance amplifier with an input resistor converting input voltage into current.

⁸This is an abbreviation of “8-pin Small Outline Integrated Circuit”

Occasionally it was found, for particular (inexplicable) values of the positive and negative power supply voltages, and particular values of the amplitude and DC offset of the function generator, that an output signal which was a distorted but recognizable version of the input sine wave could be observed. Such output signals were always lower in amplitude than the input signal itself. Moreover, the particular combinations of voltages which produced such signals were seldom reproducible.

Based on suggestions from others in the group, the UBC Physics Electronics Lab, and the op amp's datasheet [2], it was decided that RF (radio-frequency) design techniques would need to be taken into consideration.⁹ Of most concern were the lengths of the connections on and to the breadboard from the op amp. However, simply moving the breadboard components closer and shortening the wires had little effect.

It was suggested that the breadboard power supply might be responsible for the oscillations, and that an oscilloscope check of the power supply with the amplifier circuit in operation would be informative. Indeed, it was discovered that, when comparing the output of the op amp with the power supply voltages, there were large oscillations of the power supply voltage that were correlated with the amplifier output. However, correlation does not (necessarily) imply causation, and it was never determined conclusively whether the power supply caused the amplifier to oscillate, or vice versa, or whether the two acted together in producing the oscillations.

2.2.2 RF Design Modifications

In order to eliminate any effects due to poor RF design, a new op amp circuit was set up on another Surfboard, only this time, the power supply ferrites and decoupling capacitors were soldered directly to the Surfboard, as close to the op amp as possible. The purpose of the ferrites in series with the power lines is to block (or at least attenuate) any RF pickup from the power supply lines; the decoupling capacitors between the power lines and ground provide additional power supply noise rejection by shunting high-frequency power spikes to ground, and "filling in" high-frequency power dips. By placing the supply filtering close to the op amp, the length of wire between the filters and the op amp over which parasitic RF signals can be accumulated is decreased dramatically.

Additionally, a thin copper sheet was superglued to the back of the breadboard, which was to act as a ground plane. All of the ground connections on the board were soldered to this ground plane, which was in turn connected to the ground of the breadboard power supply. This is a common RF design technique which is intended to shield the circuit from noise, as well as to reduce the effects of ground loops.¹⁰ By making short connections to a large conductor acting as a common ground, such ground loop problems are kept to a minimum.

⁹Some good RF design references include the books by DeMaw [3] and Everard [5].

¹⁰Ground loops occur where wires connecting components in (or between) circuits to a common ground are long enough to act as large antennae, which are prone to receiving RF pickup. See [9] for a good reference.

The new circuit was assembled on the breadboard, on which the input and feedback resistors still remained, since it was found to be topologically impossible to connect a surface mount resistor across the op amp, using the traces on the Surfboard. When this circuit was tested, the output was improved immeasurably—the output signal always followed the input signal, with no power supply tweaking necessary—yet the output was still quite noisy, and the gain was incorrect (as the output signal amplitude was smaller than that of the input signal).

This situation was finally rectified when the input and feedback resistors (through-hole, not surface mount) were soldered directly to the Surfboard, with the feedback resistor's leads allowing it to connect above and across the op amp. With the feedback components closer to the op amp, and with no remaining unfiltered connections to the breadboard, the circuit finally worked properly, with the proper voltage gain of -20, and with significantly reduced noise. Further testing showed no problems, with the exception of some instability at low frequencies (below 1 kHz), which was determined to be an issue with the function generator and not the amplifier.

2.3 Building the Single-Stage Photodetector

After satisfactorily testing the OPA686 operational amplifier in an inverting amplifier configuration, a complete prototype of the photodetector unit was ready to be built. Assembly of the circuit was to involve more than just soldering the components to the printed circuit board (PCB); the boards themselves were to be processed in the lab as well.

Although there are other methods of making PCB's, the most accessible method for "homemade" board making involves a light exposure method, similar to development methods used in photography. The boards to be processed have a layer of copper on each side of the board, covered in a light-sensitive chemical resist layer. When an area of the board is exposed to ultraviolet light (a fluorescent light works well), the chemical resist becomes vulnerable to the developer chemical (in this case, NaOH), and immersing the board in the developer removes the exposed resist. Finally, exposing the board to a chemical etchant (this lab uses ammonium persulphate) removes all copper that is no longer protected by the resist.

After rinsing the board in water to remove the caustic (and poisonous) etchant, the development process is complete, with copper wires remaining where the board was not exposed to light. Thus by placing a standard laser-printed transparency over a board as a mask while exposing the board, the copper "trace" of a circuit may be transferred to a board. For two-sided boards, both sides of the board are exposed before developing. The only added difficulty in processing two-sided circuit boards is the need to align both sides of the board exactly opposite each other, which can sometimes be a difficult task.

For this photodiode amplifier circuit, a single-layer board transparency mask, containing 16 circuits, had already been created by the designer [8], thus there was no need to design a new mask. The first test board to be processed was

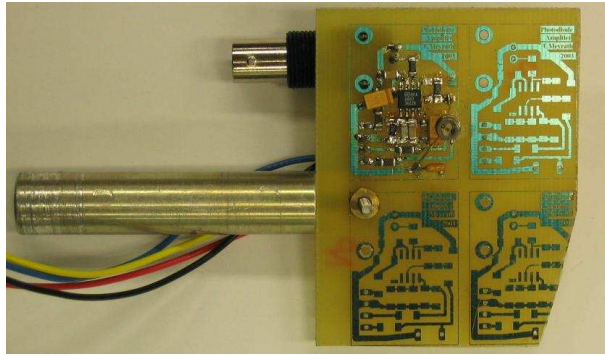


Figure 4: An assembled photodiode amplifier.

slightly overdeveloped; a second try produced a board that was good enough for assembly. Using a drill press, holes for the power supply wires and the BNC leads and supports were drilled, and then segment of the board was cut off from the rest, upon which a circuit was assembled.

The circuit was built in accordance with the original design (see Figure 2), using a Hamamatsu S5973 photodiode and a feedback resistance of $10\text{ k}\Omega$, but with no feedback capacitor to begin with. Except for the photodiode and the board-mounted BNC, most of the components were in surface mount packages. For the resistors, capacitors, and ferrites, this required no special soldering techniques¹¹ other than the use of tweezers to hold the component in place during soldering. For the op amp's eight small pins, two pins at opposite corners were soldered first, after which the rest of the pins were easily soldered; however, the pins were often found to make poor contact with the copper pads of the PCB, and a hot air rework station was used to force the solder to "flow" up the pins from the pads.

After the photodiode amplifier circuit had been assembled (see Figure 4), it was mounted on a metal post and connected to a power supply (and to the oscilloscope), and a brief, qualitative test of the photodetector was performed. An LED in series with a current-limiting resistor was connected to a function generator; by placing the modulated LED in front of a photodiode, a clean, low-noise signal was observed from the detector, whose response appeared to be quite linear.

2.4 Measuring the Frequency Response

2.4.1 Initial Attempts with an LED

One of the most important steps in the construction of the detector was an evaluation of its frequency response. Although preliminary calculations using

¹¹For an excellent online guide to surface mount soldering, see [4].

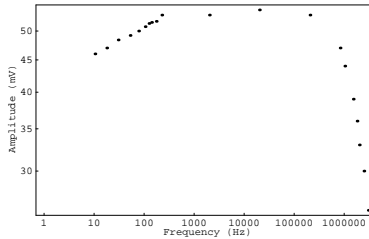


Figure 5: The original 10 kΩ frequency response data taken with the LED.

formulae in [8] and [2] predicted a bandwidth¹² on the order of 80 MHz, the parasitic capacitances and resistances of the circuit could not be determined very accurately. To rule out a bandwidth that was orders of magnitude below (or above) predictions, a measure of the actual bandwidth was desired.

For the frequency measurements, a more permanent LED signal tester was built, by drilling holes in a bent aluminum sheet, in which were mounted a BNC and a red LED. A 50 Ω current-limiting resistor was connected between the BNC signal wire and the anode of the LED, with the cathode connected through a wire to the BNC ground. This was initially modulated with the only available 3 MHz function generator, despite being incapable of reaching the predicted bandwidth.

Surprisingly, a drop-off in amplitude was observed even in the low (2–3) MHz range (see Figure 5). Since the function generator that was used only had a range of 3 MHz, it was deemed most likely to be a problem with the function generator in its highest range. A different function generator with a range of 20 MHz¹³ was obtained for further testing, so as to rule out this possibility.

Three frequency response data sets were taken with the new function generator: one for the original 10 kΩ feedback resistor, and one each after the feedback resistor had been replaced with values of 20 kΩ and 5 kΩ. While the bandwidth of the detector is supposed to decrease by a factor of $\frac{1}{\sqrt{2}}$ for each doubling of the feedback resistance R_f , the bandwidths stayed roughly the same—around 3 MHz—for all values of the feedback resistance (see Figure 6). This strongly suggested—since the function generator had been tested—that the LED itself has a bandwidth of 3 MHz; a quick measurement of the LED’s frequency response using a fast commercial detector (the Thorlabs PDA155) confirmed this fact.

2.4.2 Testing with a Laser Diode

In order to provide an accurate measurement (or even an estimate) of the bandwidth and frequency response of the detector, a different modulated light source

¹²Here, the bandwidth is defined as f_{-3dB} , which is the frequency at which the output amplitude drops to $\frac{1}{\sqrt{2}}$, or -3 dB, below the maximum.

¹³Although it was marked as 20 MHz, it worked up to almost 25 MHz.

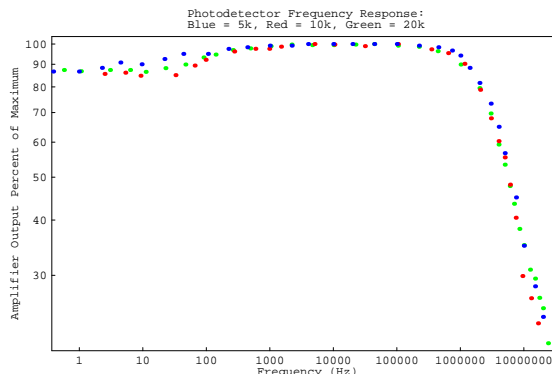


Figure 6: Frequency response data taken with the LED: Points are blue for $R_f = 5\text{ k}\Omega$, red for $R_f = 10\text{ k}\Omega$, and green for $R_f = 20\text{ k}\Omega$.

would need to be obtained. For this purpose, a 5 mW laser diode was used, initially connected through current-limiting resistors directly to the faster function generator. The function generator was set up with a small amplitude riding on a large DC offset, such that the light modulation was always in the linear regime of the laser’s “Intensity vs. Voltage” function.

Since the Thorlabs PDA155 photodetector had a known bandwidth of 50 MHz, it was used to test the combined frequency response of the laser diode and function generator. The output of the function generator was also monitored on the oscilloscope, using a $1\text{ M}\Omega$ input impedance so as to minimally perturb the signal through measurement. When the Thorlabs detector’s output was observed at different modulation frequencies, the amplitude started to decline around 14 MHz; however, the output amplitude of the function generator also showed this same decline. When the Thorlabs detector was replaced with the lab-built detector, the same response was observed. No “rolloff” was observed in either case that could not be attributed to the laser diode-function generator circuit, suggesting that the bandwidths of both detectors were somewhat higher than 25 MHz. The bandwidths of the detectors were too high to be measured with the available equipment.

2.4.3 Comparison with a Commercial Detector

Since the bandwidth of the photodetector was known to be at least 25 MHz, and knowing that the intended uses of the photodetector would seldom require a bandwidth greater than several megahertz, the bandwidth of the photodetector was declared to be more than sufficient. However, while an exact measurement of the bandwidth of the detector was deemed unnecessary, it was decided that a side-by-side comparison of the performance of the lab-built detector with that of the Thorlabs detector would be informative.

In order to compare the performance of the two detectors with the same

signal, a glass microscope slide was positioned with a large angle of incidence in the beam, acting as a simple beam-splitter. The angle was adjusted to roughly equalize the split beam intensities. The Thorlabs detector was placed in the reflected beam, while the transmitted beam was reflected off two mirrors towards the other detector.

To drive the laser diode, a new technique was used; the function generator still provided the DC offset, but the modulation was provided by a recently obtained Agilent 8648A RF Synthesizer, which could modulate up to 1 GHz. Both sources were connected to the laser diode via an improvised circuit board, on which the RF synthesizer was connected through a $50\ \Omega$ resistor and 1 nF capacitor to protect it from the DC offset, and the function generator was connected through ferrite beads to protect it from the modulation.

The idea behind testing the two detectors simultaneously was to negate the frequency dependency of the laser's modulation amplitude. Where the responses of the detectors are linear, both will observe the same proportional variations of the light modulation, and the ratio of the detector outputs will remain constant. Assuming the detectors have different bandwidths, the ratio of the detectors' output amplitudes will change when one detector's output begins to drop faster than the other; a second change will be observed where the faster detector's response declines as well. This gives some indication of the bandwidths of the detectors.

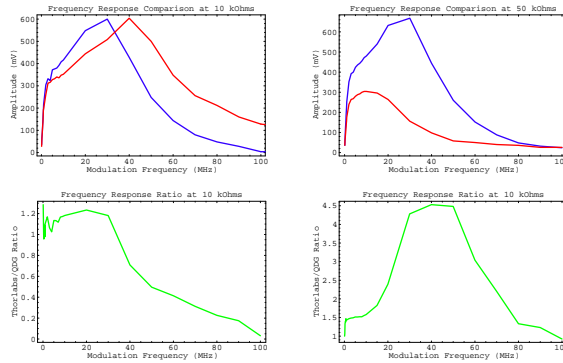


Figure 7: The results of the comparison with the Thorlabs detector. $R_f = 10\ \text{k}\Omega$ on the left and $50\ \text{k}\Omega$ on the right; the lab detector amplitudes are in red, Thorlab amplitudes are in blue, and ratios are in green.

When the measurements were taken with a feedback resistance of $10\ \text{k}\Omega$, the lab-built detector clearly outperformed the Thorlabs detector (see Figure 7, left); it reached its peak near 40 MHz, 10 MHz after the Thorlabs detector, and while the Thorlabs detector's amplitude drops to near zero by 100 MHz, the lab-built detector maintains an amplitude above 50 mV out to 250 MHz!

For a feedback resistance in the lab-built detector of $50\ \text{k}\Omega$, the situation is

reversed (see Figure 7, right); the Thorlabs detector significantly outperforms the lab-built detector¹⁴. The behaviour is as expected, since the increase in feedback resistance by a factor of 5 should scale the frequency response by $\frac{1}{\sqrt{5}}$; the increase in the amplitude ratio near 20 MHz corresponds to the “rolloff” of the lab-built detector, roughly $\frac{1}{\sqrt{5}}$ lower than its 45 MHz rolloff with $R_f = 10 \text{ k}\Omega$.

Having tested the frequency performance of the photodetector for both feedback values, it was decided that the 10 k Ω feedback resistance provides the best compromise between gain and bandwidth. This will be the value chosen for future photodetector units to be assembled.

2.5 Conclusion

The initial goal of constructing and testing a general-purpose photodetector appropriate for most laboratory uses appears to have been met. The small size of the circuit (with 16 circuits fitting on a board) will allow the photodetectors to be placed whatever tight spaces may be necessary. Additionally, the very high bandwidth (around 45 MHz for $R_f = 10 \text{ k}\Omega$) is orders of magnitude greater than what will be required for most situations, and should be sufficient for any high-frequency monitoring applications which may arise. With the exception of the design of a metal enclosure to protect and mount the circuit, only the “mass production” phase of the single-stage photodetector project remains.

¹⁴Note that a neutral density filter was used to attenuate the beam for the 50 k Ω lab-built detector; however, this only scales the ratio by a constant factor.

3 The Dual-Stage Photodetector

3.1 Introduction

During the construction, testing, and evaluation of the original detector design, it was decided that a separate photodetector model should be built for the saturated absorption monitors, to be used in the laser locking system (see Appendix B). The signals which the locking system photodetectors will be monitoring will be small modulations of around 100 kHz, on top of a steady light intensity, with the modulation typically being only 1% of the steady intensity. Such a signal is ill-suited for use in the locking system, which really only “cares about” the modulation.

A better detector for this purpose would only amplify the modulation for its output. The simplest way to achieve this is to use two amplification stages: the first to amplify the DC signal to usable levels for DC filtering, and a second to amplify only the remaining modulation. This is the basic design of the dual-stage photodetector that was constructed in this report.

In addition to the photodetector circuit itself, a metal enclosure for the detector was designed and submitted to the UBC Physics Machine Shop to be machined. This will not be covered in the body of the report below, but an overview of the enclosure may be found in Appendix C.

3.2 The Circuit Design

The design of the dual-stage photodetector was based on a combination of two separate designs: the original single-stage design [8], and a dual-stage photodetector designed by the JILA Electronics Lab [7]. The DC stage of the detector was to be the same as the original one-stage design. The AC stage, however, would consist of a high-pass RC filter¹⁵ after the output of the DC stage, connected into the input of a non-inverting amplifier (see Appendix A.4).

The operational amplifier that was chosen for the AC stage was the Analog Devices AD829, which has a gain-bandwidth product of 750 MHz. Incidentally, between the time that the OPA686 was ordered for the original detectors and the ordering of parts for the new detectors, the OPA686 was to be declared by Burr-Brown to be nearing obsolescence, and was no longer recommended for new use. Fortunately, there was a recommended replacement op amp, the Burr-Brown OPA846, that was almost exactly equivalent, but with a higher gain-bandwidth product of 1750 MHz; this was the op amp that was chosen for the DC stage of the dual-stage detectors, as well as for future production of the single-stage detectors.

One feature that was to be built into the new detectors was the ability to switch the output between the AC and DC stages; that is, the ability to “turn off” the AC amplification stage, and divert the output of the DC stage directly to the BNC (but through a 50 Ω output resistor for impedance matching, as before).

¹⁵An RC high-pass filter consists of a capacitor in series with the line, and a resistor to ground. Such a filter blocks low frequencies, with a rolloff at $f_{-3dB} = \frac{1}{2\pi RC}$.

This would not only allow the absolute DC intensity of the saturated absorption pump and probe beams to be checked, it would also allow the detectors to be used for general purpose light detection when necessary. To implement this, the output of the DC stage would need to be switched between the AC stage input and the BNC, and the AC stage output would also need to be simultaneously switched between the BNC and somewhere else. If the AC stage output is not disconnected from the DC stage while its inputs are disconnected, it may introduce its own noise, offsets, or oscillations to the DC output, which would be undesirable. In order to switch both connections, a double-pole double-throw¹⁶ was necessary.

Another feature which was desired was the ability to adjust the value of the gain for the AC stage. This would be made possible through the use of a potentiometer as part of the feedback resistance of that stage. Another resistor in series with the potentiometer would be necessary to maintain a minimum gain of 20, since the AD829 was identified in its datasheet as being unstable for gains smaller than this value. The AC stage was designed to use a 20 k Ω potentiometer in series with a 3.8 k Ω resistor for the feedback loop, and a 200 Ω resistor to ground. Using Equation 7 derived in Appendix A.3, the minimum gain is:

$$G_{min} = 1 + \frac{R_{f,min}}{R_g} = 1 + \frac{3.8 \text{ k}\Omega}{200 \Omega} = 1 + 19 = 20 \quad (1)$$

And the maximum gain is:

$$G_{max} = 1 + \frac{R_{f,max}}{R_g} = 1 + \frac{23.8 \text{ k}\Omega}{200 \Omega} = 1 + 119 = 120 \quad (2)$$

A 20 k Ω “offset trim” adjustment potentiometer was also included for the AD829, to make use of its offset adjustment pins. This potentiometer takes a -15 V supply input to its center pin, with the two outside pins connected to the offset adjustment pins of the AD829. This configuration “splits” the -15 V supply between the two pins, with one pin receiving x Volts and the other receiving $15 - x$ Volts. The offset trim control is optional, and in future construction of the dual-stage photodetector, it may be omitted, but in case it is found to be necessary, the option to include it should be built into the board.

Finally, for the DC stage, a constant feedback resistance (and transimpedance gain) of 50 k Ω was chosen. Although this results in a smaller bandwidth than if a 10 k Ω resistor was used, this bandwidth is still around 20 MHz, which is at least two orders of magnitude greater than the approximately 100 kHz modulation the detectors were designed to observe. The sacrificed bandwidth will result in a gain (and thus a signal) which is five times larger, which may sometimes require optical attenuation to avoid saturating the DC amplification stage. This occasional need for attenuation does not outweigh the benefit of being able to observe signals which are five times weaker, as it is usually much harder to increase a weak signal strength than to attenuate a strong one.

¹⁶Or “DPDT”: essentially, a switch controlling two separate lines (poles), with two possible connections (throws) for each line.

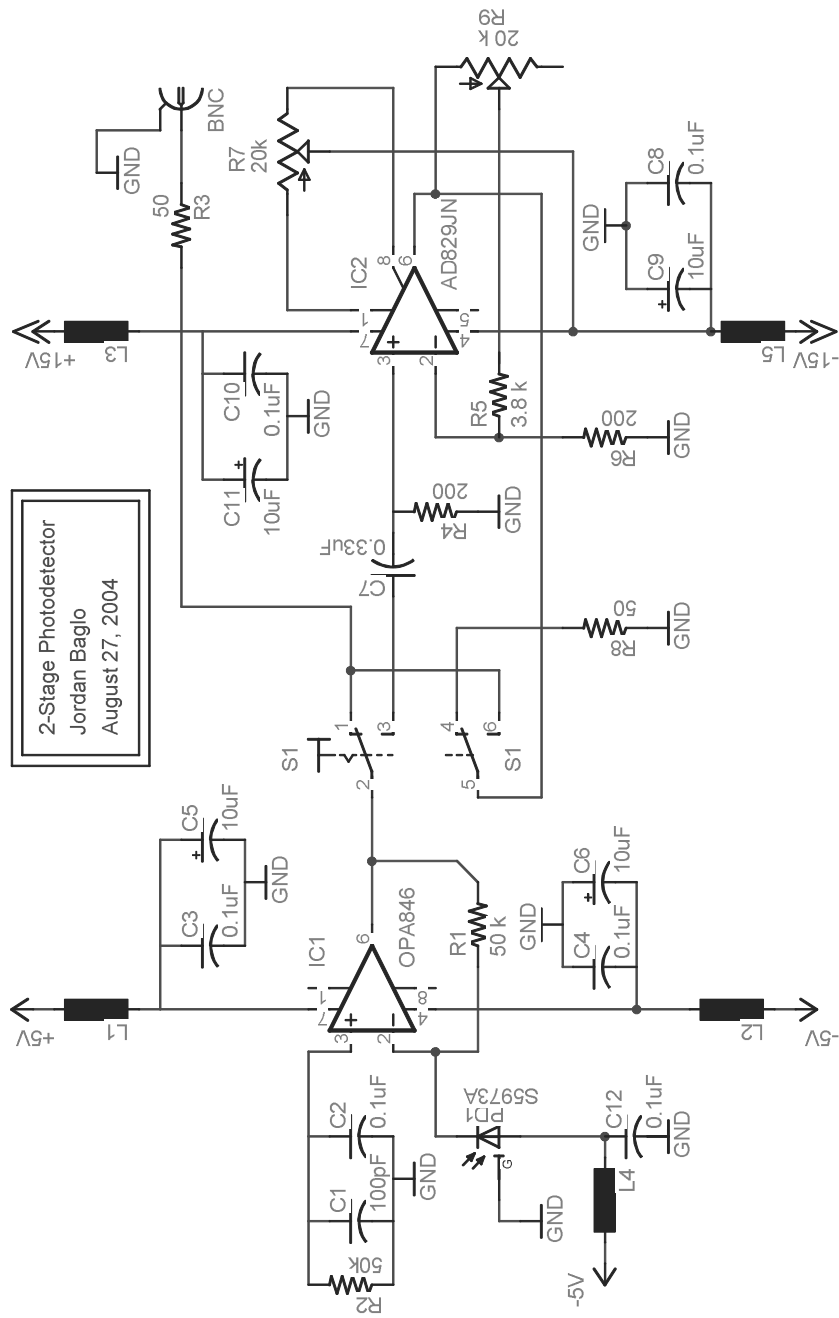


Figure 8: The dual-stage photodetector schematic.

The schematic for the complete circuit design, combining all of these design specifications, is shown in Figure 8.

3.3 The Board Layout

In order to construct this circuit, a circuit board would need to be laid out, according to the design. The main program that was used to design the circuit board (and draw the schematic) for the dual-stage photodetector was EAGLE, an electronics design suite produced by CadSoft.

Before designing the board, there were several decision to make regarding the physical composition of the circuit. The most important decision was whether to use surface mount or through-hole components on the board. In some cases, there was little choice; the OPA846 is only available in surface mount form, and the BNC, the photodiode, and the wires from the board to the panel mount DIN power connector would require through-holes to be drilled. For the remainder of the components, there was a choice between the two package types which needed to be resolved.

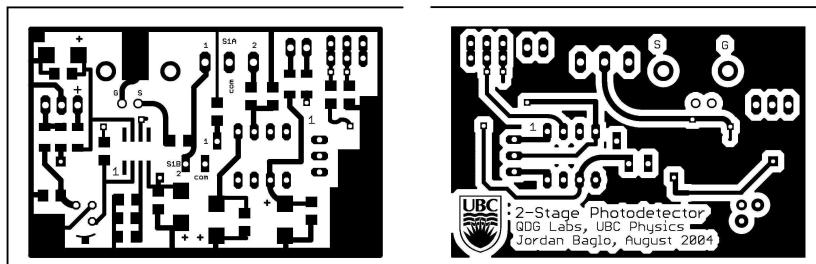


Figure 9: Both sides of the printed circuit board copper trace for the dual-stage photodetector. The top side is on the left.

In the interest of building a compact board that would be more convenient for laboratory use, all of the capacitors and fixed-value resistors on the board—which comprise the bulk of the circuit—were chosen to have surface-mount packages. This allowed many such passive components to be squeezed into relatively small space on the board. The choice of surface mount packages for the fixed-value passive components would also reduce the noise that would otherwise be introduced into the circuit from the added path lengths through the larger components, which can be especially problematic in the feedback paths of the op amps. For the potentiometers, though surface mount packages are available, the extra structural support provided by through-hole pins was deemed important, particularly for the AC gain adjust, which would be pressed on with a screwdriver during adjustments. Finally, a through-hole DIP (dual in-line pin) package was chosen for the AC stage AD829 op amp. The main reason for using a through-hole op amp package was to allow the op amp to be inserted into a socket on the board, rather than being soldered directly to it; the

suitability of the AD829 op amp for this photodetector circuit was not certain, and a socket would allow the replacement of the op amp during testing.

Once the components were chosen, the circuit board layout was designed in EAGLE. Since the circuit board needed to be as small as comfortably possible (with regards to assembly), several iterations of the design process were necessary before a satisfactory board layout (which was 2.20" long and 1.45" wide) was obtained. The circuit board trace for the final layout is shown in Figure 9.

The main difficulty encountered during the design of the board layout was the familiar problem of connecting components without crossing traces. Often this problem was resolved through the use of "vias," which are connections from one side of the board to the other, made by inserting a wire into a hole in the board which is soldered to pads on both sides. This allowed wires to avoid obstacles on one side of board by crossing under (or over) them on the other side. This technique greatly simplified the layout process, as many connections were made between opposite sides of the board.

3.4 Building the Dual-Stage Photodetector

After the board layout was finalized (at least for the short term), a transparency mask was printed, with five copies each of the top and bottom traces of the circuit. These traces needed to be aligned on the transparency so that the top and bottom of the circuits would line up exactly after the boards were etched; the creation of the board mask transparency was done in VectorWorks, a CAD program with decent layout and measurement capabilities, so as to ensure exact alignment.

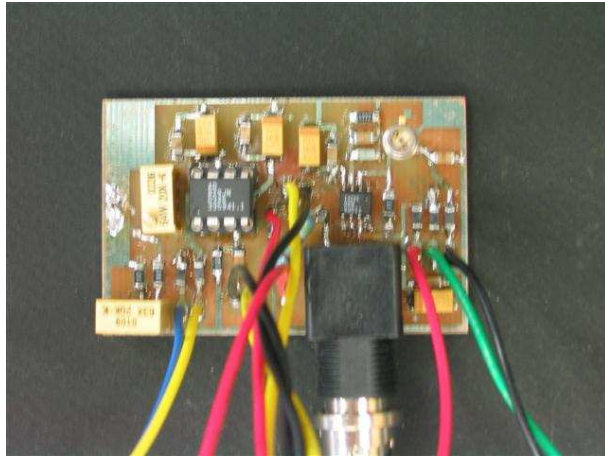


Figure 10: A fully assembled dual-stage photodetector board.

Having printed the transparency, a circuit board containing five copies of the dual-stage photodetector was developed. The board development process

was the same as described earlier in 2.3, except for the second side of the board which needed to be exposed; the details need not be repeated here. All five boards were cut and drilled, in preparation for soldering and assembly. Finally, the components for one board were assembled and soldered, and a prototype of the dual-stage photodetector unit was complete (see Figure 10).

3.5 Conclusion

At the time of the conclusion of this report, only very basic tests have been carried out with the two-stage detector. While the DC stage works as well as before, the AC stage is quite prone to noise and oscillation. Removing the socket and soldering the op amp directly to the board may fix the problem, but it may be necessary to simply use a slower op amp to remove high-frequency oscillation. However, when an LF411 op amp—a much slower operational amplifier, with a gain-bandwidth product of only 3 MHz—was substituted for the AD829, the noise and oscillations disappeared, for the most part. This was, however at the cost of speed, and the LF411 was unable to amplify even signals at 100 MHz with any appreciable amplitude.

In conclusion, while a prototype of the dual-stage photodetector has been successfully designed and constructed, more work needs to be done to ensure the stability of the detector. It seems that a compromise between speed and stability must be made, and will need to be decided before the remainder of the dual-stage photodetector units are built.

Appendices

A The Operational Amplifier

Aside from discrete components such as resistors, capacitors, and diodes, the operational amplifier is quite possibly the most useful and versatile electronic component ever to grace a circuit board. Originally developed to perform mathematical operations—including differentiation and integration—in analog computers (hence the name), operational amplifiers today continue to form the backbone of analog circuitry.

A.1 Basic Uses and Properties

The operational amplifier is essentially a differential amplifier with a very high open-loop voltage gain A_{OL} , typically in a monolithic (integrated circuit) package. As a differential amplifier, the op amp (as it is commonly named) uses as its output the amplified difference of its inverting and non-inverting input voltages (V_- and V_+ , respectively):

$$V_O = A_{OL}(V_+ - V_-) \quad (3)$$

Due to the large value of A_{OL} for the op amp (for the Burr-Brown OPA846 used in this project, for example, $A_{OL} = 90 \text{ dB} = 3.16 \times 10^4 \text{ V/V}$), extremely small differences (only $104 \mu\text{V}$ for the OPA846) between the input voltages will send the op amp’s outputs to its maximum output voltage.¹⁷ This property allows the operational amplifier to be used as a *comparator*, whereby the op amp’s output is positive when the difference $V_+ - V_-$ is positive, and the output is negative when the difference is negative; This is a useful application in its own right.

A.2 Negative Feedback and the “Golden Rules”

However, the most useful applications of the operation amplifier occur where some of the output voltage is fed back to its inverting input; when the noninverting input is more positive than the inverting input, a positive voltage from the output is fed back to the inverting input, reducing the difference between the inputs, and thus reducing the output. For an appropriate feedback path, this negative feedback forces the output to a stable equilibrium. The operational amplifier is most commonly used with some such form of negative feedback.

When analyzing circuits using operational amplifiers with external feedback, it can be extremely helpful (and informative) to make use of two basic principles of their operation, popularized as the “Golden Rules” of op amp behaviour by Horowitz and Hill in their popular book, *The Art of Electronics* [6]. In the original words of those authors, the rules are as follows:

Rule 1 *The output attempts to do whatever is necessary to make the voltage difference between the inputs zero.*

¹⁷This is always less than, but usually close to the operational amplifier’s supply voltage. The positive and negative supply voltages of the op amp are commonly referred to as its *rails*, and thus an op amp which can output all the way to its supply voltage is known as *rail-to-rail*.

Rule 2 *The inputs draw no current.*

Although these rules are only approximations, they hold up exceptionally well in most all cases, especially for the purposes of basic design and analysis. For example, Rule 2 is not exactly correct, as the input impedance of the op amp is finite, not infinite, thus some current must be drawn with applied voltage. However, for most op amps, this input impedance is very large: on the order of megohms for op amps with bipolar transistor inputs, and sometimes greater than 10^{12} ohms for those with field-effect transistor (FET) inputs! The associated input currents are generally on the order of nanoamps, down to picoamps for the FET-input variety, and can often be safely ignored in analysis.

A.3 The Inverting Amplifier

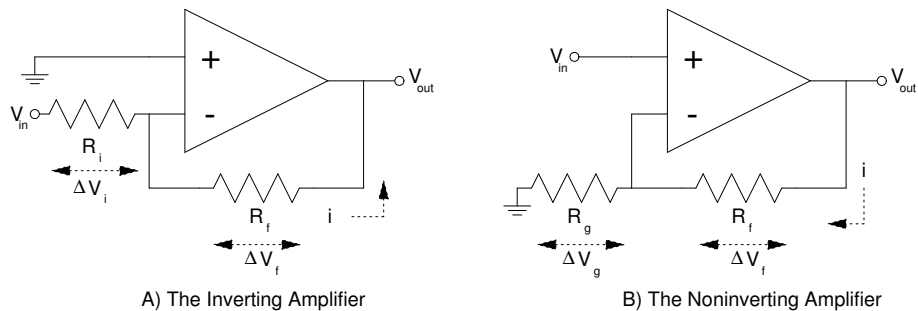


Figure 11: The two most common op amp configurations, the inverting (A) and non-inverting (B) amplifiers. Current directions are for positive V_{in} .

The two most basic configurations of the operational amplifier are known as the inverting and noninverting amplifiers. Expressions for the closed-loop voltage gains G (for an ideal op amp) in terms of their component resistors can be easily derived using only the golden rules and Ohm's Law.

For the inverting amplifier (see Figure 11A), according to the first Golden Rule, the op amp should output the necessary current such that the voltage at its inverting input (V_-) is equal to that at its noninverting input (V_+), which is set to ground. This forces the voltage change ΔV_i across the input resistor R_i to be equal to the full voltage V_{in} measured with respect to ground; that is, $\Delta V_i = V_{in}$. The current I through this resistor which corresponds to this potential difference is $I = \frac{-\Delta V_i}{R_i}$.

Since, by the second Golden Rule, none of this current will pass through the op amp, this entire current will pass through the feedback resistor R_f , generating

another potential voltage difference, which will be negative for positive input voltages V_{in} . Since V_- is at $V = 0$, the output voltage V_{out} will be this entire potential drop $-\Delta V_f$ below ground, or:

$$V_{out} = -IR_f = \left(\frac{-\Delta V_i}{R_i} \right) R_f = \frac{-R_f}{R_i} \Delta V_f \quad (4)$$

Which simply becomes the expression for the closed-loop gain G :

$$G = \frac{V_{out}}{V_{in}} = \frac{-R_f}{R_i} \quad (5)$$

A.4 The Noninverting Amplifier

A derivation of the closed-loop gain for the noninverting amplifier proceeds in a very similar manner. Using the first golden rule," we can express the inverting input voltage V_- in terms of the non-inverting input voltage V_+ , which is set to be V_{in} . The voltage drop across the resistor R_g from the noninverting input to ground is thus equal to the input voltage V_{in} , corresponding to a current of $I = \frac{V_{in}}{R_g}$ to ground through this resistor.

Once again, we may use the second Golden Rule (and Kirchhoff's Law of Currents) to require that the current through the feedback resistor R_f be equal to the current through the ground resistor R_g . For a positive input voltage, there is a negative voltage drop across R_g to ground, causing the current flow in R_g to be towards ground, and therefore causing the current flow in R_f to be from the output of the op amp towards ground. This current corresponds to a voltage change $\Delta V_f = IR_f$ from the inverting input to the output, with the current I being towards ground. Thus the output voltage can be expressed as:

$$V_{out} = V_- + \Delta V_f = V_{in} + IR_f = V_{in} + \left(\frac{V_{in}}{R_g} \right) R_f \quad (6)$$

And thus the expression for the closed-loop gain G is:

$$G = \frac{V_{out}}{V_{in}} = 1 + \frac{R_f}{R_g} \quad (7)$$

B The Laser Lock System

The laser locking system that will incorporate the photodetectors described in this report uses the techniques of Doppler-free saturated absorption spectroscopy and phase-sensitive detection to provide the necessary feedback loop to lock the laser wavelengths to the desired atomic line. This appendix will provide a (very) brief and qualitative description of these techniques—without going into much detail and without the use of any equations—which was found to be too long for the main text of this report.

B.1 Doppler-free Saturated Absorption Spectroscopy

Standard absorption spectroscopy involves the use of a single laser beam passing through a gas cell, with the absorption at each wavelength determined from the intensity of the beam that has passed through the cell. Due to the thermal distribution of velocity of the gas atoms inside the cell, each atom will “see” its lines at Doppler-shifted wavelengths, and the absorption lines will be *Doppler-broadened*, preventing accurate measurements of the atomic line.

One way to circumvent this broadening is to use two counterpropagating laser beams of the same frequency—a pump beam and a probe beam—with one beam (the pump beam) being more intense than the other. With the two beams aligned in such an antiparallel configuration, only the atoms moving entirely orthogonal to the beams will see both beams at the same unshifted frequency, as any atom with a transverse velocity will see the beams with different frequencies.

When the pump beam is sufficiently intense that the excited state whose transition corresponds to a given line has been saturated, such that the atoms can absorb no more photons at that frequency for the lifetime of the state, then the probe beam will see an decrease in absorption at that frequency. The photodetectors described in this report will measure the intensity of the pump and probe beams, and the difference of the probe beam signal from the pump beam signal (provided by the photodetectors) will show a “Lamb dip” at the correct atomic lines, unbroadened by Doppler shifts. This is known as Doppler-free saturated absorption spectroscopy [11].

B.2 Phase Sensitive Detection

While this saturated absorption spectroscopic technique alone is sufficient for observation of atomic lines, this experiment requires not that we observe such lines, but that we lock the frequency of our laser to them. In order to actually lock the beams to the line, a modification of the setup is required.

To provide the locking of the beams, the frequency of the laser light is modulated by passing it through an acousto-optic modulator (AOM). In the AOM, light Bragg-diffracts off of acoustic waves in a crystal, generated by a piezoelectric element (a piezo). The diffracted beam separates (spatially) into discrete diffraction orders, whose frequencies are determined by the modulation of the

piezo. By selecting one such diffraction order, and varying the modulation of the piezo, one may modulate the frequency of the lasers.

For the locking system, the frequencies of the pump and probe beams are together modulated (using the AOM) over a small range¹⁸ back and forth. The same saturated absorption technique is applied with the modulated beams, and the inverse of the difference of the probe beam signal from the pump beam signal is considered, such that a peak (rather than a Lamb dip) is observed at the atomic resonance. When the “center frequency” of the two beams before modulation is slightly below the atomic line, and when the modulated frequency is increasing, the inverted difference signal is also increasing, and vice versa; that is, the signals are in phase. The converse is true for center frequencies above the atomic line—the signals have opposite phases.

When these signals are multiplied electronically, the result is positive (since the signals are in phase) for laser frequencies below the line, and negative for those above the line. This technique, known as phase sensitive detection, gives the required direction the wavelength needs to change, and provides the feedback necessary to lock the lasers to the line.

¹⁸Around 100 kHz, compared to the atomic line width of several MHz

C The Photodetector Enclosure

As part of the photodetector construction project, it was also necessary to design an enclosure for the detectors in addition to the electronics. The design (which is shown below, in Figures 12–17) was submitted to the UBC Department of Physics Machine Shop, where the components of the enclosures were machined.

The enclosures were designed after the PCB layout was finalized. The dimensions and placement of the holes in the panels were carefully determined, based on both the placement of components on the PCB board and the dimensions of the components as specified on their manufacturers' data sheets. The board is designed to mount on the front panel using the board-mount BNC connector; the board will be prevented from turning inside the enclosure by virtue of the special D-shaped hole on the panel, which does not allow for rotation of the BNC.

The enclosure is a rectangular box, built from six panels held together by 4-40 UNC screws. There are only five different panel types, as both side panels are identical. Each panel is constructed from 1/4" black anodized aluminum; the panels were anodized mostly for aesthetic reasons.

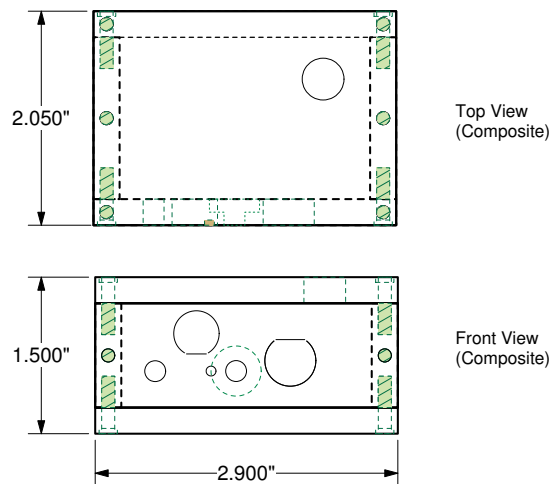


Figure 12: Photodetector enclosure design, overview

Photodetector Enclosure: Bottom Plate

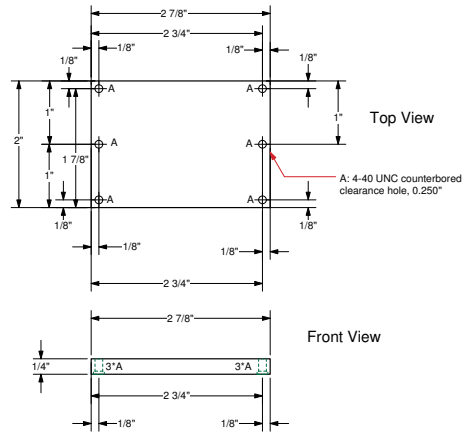


Figure 14: Photodetector enclosure design, bottom plate

Photodetector Enclosure: Top Plate

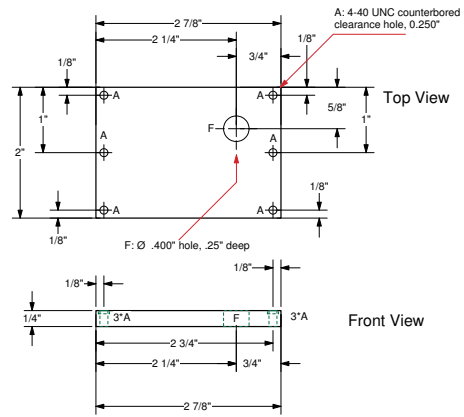


Figure 15: Photodetector enclosure design, top plate

Photodetector Enclosure: Rear Plate

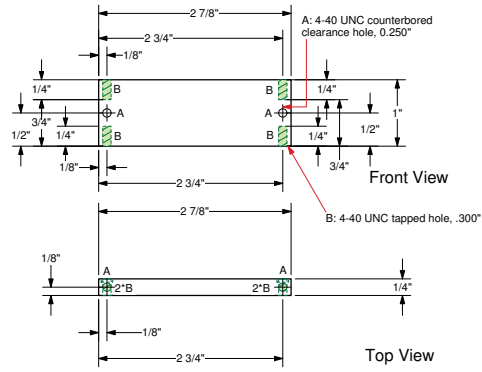


Figure 16: Photodetector enclosure design, rear plate

Photodetector Enclosure: Side Panels

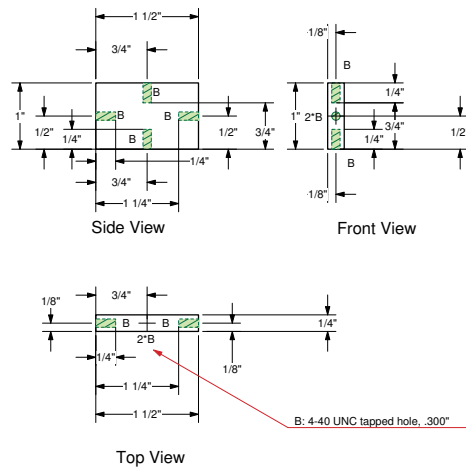


Figure 17: Photodetector enclosure design, side panels

D List of Equipment

The following list is not an exhaustive compilation of everything that was used, but rather a list of the products and equipment were most important or most relevant throughout the design, testing, and construction of the photodetectors.

D.1 Design and Data Analysis Software

Product	Brand & Model
Electronics design	Altium (Protel) CircuitStudio 2004
Electronics design	CadSoft EAGLE Light Edition 4.1
Electronics/mechanical design	MiniCAD VectorWorks 8.5.2
Data analysis	Wolfram Research Mathematica 4

Table 1: Software used for design, layout, and data analysis.

D.2 Electrical/Optical Measurement Equipment

Product	Brand & Model
Digital multimeter	Extech Instruments 380282
Digital oscilloscope	Tektronix TDS3014
High-speed photodetector	Thorlabs PDA155
Laser power detector	Coherent FieldMaster-GS
Optical spectrum analyzer	Ando AQ-6315A

Table 2: Equipment used for electrical and optical measurements.

D.3 Laser Equipment

Product	Brand & Model
Helium-Neon laser	1 mW HeNe at 633 nm, unknown origin
Laser diode	NVG Inc. model D660-5, 5 mW at 660 nm
Collimation tube	Thorlabs LT230P-B collimation tube

Table 3: Laser equipment used for testing.

D.4 Power Supplies and Signal Sources

Product	Brand & Model
Function generator (3 MHz)	Interstate Electronics Corp. F33
Function generator (20 MHz)	BK Precision 4040A
Synthesized signal generator (1 GHz)	Agilent 8648A
Breadboard w/ power supply	K&H Projects PP-272
Power supply (± 15 V, floating 5 V)	Power-One CP131-A

Table 4: Power supplies and signal sources used.

D.5 Soldering and Assembly Equipment

Product	Brand & Model
Soldering iron	Weller TC201P
Soldering tip	Weller PTA8 (screwdriver)
Soldering tip	Weller PTS7 (long conical)
Soldering system	Metcal MX-500S
Soldering tip	Metcal STTC-537 (chisel)
Soldering tip	Metcal STTC-507 (conical)
Soldering tip	Metcal STTC-540 (bent)
Hot air rework station	Atten 850
Carbide drill bits	Drill Bit City, #68
Carbide drill bits	Drill Bit City, #71

Table 5: Equipment for soldering and assembling boards.

D.6 PCB Processing Equipment and Supplies

Product	Brand & Model
Etching tank, air pump, & heater	Circuit Specialists ET10 Etching System
PCB exposure fluorescent light	MG Chemicals 416-X Exposure Kit
PCB developer (NaOH)	MG Chemicals #418 Developer
PCB etchant	MG Chemicals Ammonium Persulphate

Table 6: PCB processing chemicals and equipment.

E List of Vendors

Much of the equipment and supplies used in this project were already available in the lab before the project commenced. However, all of the electronics components (as well as some equipment and supplies) used in this project needed to be ordered (and reordered). Additionally, some components (i.e. the enclosure for the photodetector) needed to be machined or manufactured. These were each obtained from the vendors, distributors, and other businesses in Table 7:

Vendor	Products / Services	URL or Location
Allied Electronics	Electronics components	http://www.alliedelec.com
DigiKey	Electronics components	http://www.digikey.ca
Electrosonic	Electronics components	http://www.e-sonic.ca
Mouser	Electronics components	http://www.mouser.com
Newark InOne	Electronics components	http://canada.newark.com
Hamamatsu	Optoelectronics	http://www.hamamatsu.com
Drill Bit City	Carbide drill bits	http://www.drillbitcity.com
UBC Physics Machine Shop	Enclosure machining	Hennings Building, UBC
UBC Physics Electronics Lab	Electronics components	Hennings Building, UBC

Table 7: A list of vendors, distributors, and other businesses used

Bibliography

- [1] Jeremy Bernstein, Paul Fishbane, and Stephen Gasiorowicz. *Modern Physics*. Prentice Hall, 2000.
- [2] Burr-Brown. *OPA686 Datasheet*, September 2000.
- [3] Doug DeMaw. *Practical RF design manual*. Prentice-Hall, Englewood Cliffs, N.J., 1982.
- [4] Luke Enriquez. Hints and tips for using surface mount technology. An online guide to SMT, found at <http://www.geocities.com/vk3em>, August 2001.
- [5] Jeremy Everard. *Fundamentals of RF Circuit Design: with Low Noise Oscillators*. John Wiley and Sons, Chichester, 2001.
- [6] Paul Horowitz and Winfield Hill. *The Art of Electronics*. Cambridge University Press, Cambridge, second edition, 1989.
- [7] JILA Electronics Lab. *2-Stage Photodetector Circuit Schematic*, June 2002.
- [8] Todd P. Meyrath. A simple photodiode amplifier. A design for a photodiode amplifier, with notes, schematics, and a PCB mask, April 2004.
- [9] John H. Moore, Davis C. Christopher, and Michael A. Coplan. *Building Scientific Apparatus: A Practical Guide to Design and Construction*. Westview Press, Redwood City, Calif., second edition, 1989.
- [10] Roberto Onofrio and Carlo Presilla. Ultracold atomic fermi-bose mixtures in bichromatic optical dipole traps: a novel route to study fermion superfluidity. *Journal of Statistical Physics*, 115(1-2):57–89, 2004.
- [11] Daryl W. Preston. Doppler-free saturated absorption: Laser spectroscopy. *American Journal of Physics*, 64(11):1432–1436, 1996.
- [12] Volker Schweikhard. *Ultracold Atoms in a Far Detuned Optical Lattice*. PhD thesis, Physikalisches Institut, Universität Stuttgart, November 2001.
- [13] Peter van der Straten and Harold Metcalf. The quest for bec. In Claus Zimmermann Matthias Weidemler, editor, *Interactions in Ultracold Gases: From Atoms to Molecules*, pages 1–63. WileyEurope, March 2003.